J Nanostruct 16(2): 1990-2002, Spring 2026

RESEARCH PAPER

Eco-Friendly Synthesis and Characterization of Silver Nanoparticles Using Orange Peel Extract: Antibacterial Efficacy Against Clinical Isolates from Burn and Wound Infections

Mohammed Ayad Shukur *, Ranea Aomed Jawaid Bajilan

Department of Medical Laboratory Techniques, College of Medical and Health Technologies, University of Bilad Al-Rafidain, Diyala, Iraq

ARTICLE INFO

Article History:
Received 09 January 2026
Accepted 23 March 2026
Published 01 April 2026

Keywords:
Antimicrobial activity
Burn infections
Green synthesis
Orange peel extract
Silver nanoparticles
Wound infections

ABSTRACT

The increasing prevalence of antimicrobial resistance (AMR) in burn and wound infections necessitates alternative antimicrobial strategies. This study explores the green synthesis of silver nanoparticles (AgNPs) using orange peel extract as a sustainable alternative to combat pathogenic bacteria. AgNPs were synthesized using orange peel extract and characterized using UV-Vis spectroscopy, X-ray diffraction (XRD), transmission electron microscopy (TEM), and Fourier-transform infrared spectroscopy (FTIR). Pathogenic bacteria were isolated from burn and wound samples, and the antimicrobial activity of the synthesized AgNPs was evaluated through inhibition zone measurements, and minimum inhibitory concentration (MIC). The synthesis was confirmed by a color change from orange to dark brown and further validated by UV-Vis spectroscopy, which showed a characteristic surface plasmon resonance peak at 418 nm. XRD analysis revealed that the AgNPs have a face-centered cubic structure, while TEM showed them to be polydisperse and spherical with an average size of 24.50 nm. FTIR identified various functional groups involved in the reduction and stabilization of AgNPs. The biosynthesized AgNPs exhibited significant antimicrobial activity against both Gram-positive and Gram-negative bacteria, including multidrug-resistant strains. The disk diffusion assay demonstrated clear zones of inhibition, with *Staphylococcus aureus* ATCC 33591 being the most sensitive strain. The minimum inhibitory concentration (MIC) for this strain was 25 µg/mL. The results highlight the potential of these green-synthesized AgNPs as effective antimicrobial agents against multidrug-resistant bacteria, offering a promising solution for addressing antimicrobial resistance challenges. This study contributes to the development of sustainable nanotechnology and provides insights into the applications of eco-friendly synthesized nanoparticles in healthcare.

How to cite this article
Shukur M., Bajilan R. Eco-Friendly Synthesis and Characterization of Silver Nanoparticles Using Orange Peel Extract: Antibacterial Efficacy Against Clinical Isolates from Burn and Wound Infections. J Nanostruct, 2026; 16(2):1990-2002. DOI: 10.22052/JNS.2026.02.046

INTRODUCTION

Burn and wound infections are a major global health concern, particularly in hospital settings, where they contribute significantly to patient morbidity, prolonged hospital stays, increased healthcare costs, and mortality [1]. Thermal injuries destroy the protective skin barrier, exposing underlying tissue to microbial colonization and infection. Opportunistic

* *Corresponding Author Email: hamaayad90@gmail.com*

pathogens, especially thosfige forming biofilms, readily invade these compromised sites, making treatment complex and challenging [2]. Burn wounds, in particular, are highly vulnerable to infections due to their extensive tissue damage and nutrient-rich exudates, which support rapid bacterial proliferation [3]. The situation is further complicated when the causative organisms display resistance to commonly used antibiotics.

Antimicrobial resistance (AMR) has emerged as one of the most pressing challenges in contemporary medicine. According to the World Health Organization, AMR is responsible for an estimated 1.27 million deaths annually and is projected to become the leading cause of death by 2050 if unaddressed [4]. Pathogens frequently isolated from burn and wound infections, such as *Staphylococcus aureus*, *Pseudomonas aeruginosa*, *Klebsiella pneumoniae*, and *Acinetobacter baumannii*, are increasingly exhibiting multidrug resistance (MDR), leaving clinicians with limited therapeutic options [5,6]. The emergence of methicillin-resistant *Staphylococcus aureus* (MRSA) and extended-spectrum beta-lactamase (ESBL)-producing *Enterobacteriaceae* further aggravates the situation, underscoring the urgent need for alternative antimicrobial agents [7].

In this context, silver nanoparticles (AgNPs) have garnered significant attention due to their potent and broad-spectrum antimicrobial activity. Unlike traditional antibiotics that typically target a specific microbial pathway or structure, AgNPs disrupt multiple cellular processes simultaneously. These include physical disruption of microbial membranes, generation of reactive oxygen species (ROS), binding to thiol groups in enzymes, and interference with DNA replication and protein synthesis [8,9]. This multi-targeted mechanism makes it substantially more difficult for microorganisms to develop resistance to AgNPs. Moreover, AgNPs have demonstrated activity not only against planktonic bacteria but also against biofilms, which are notoriously resistant to antibiotics and a major complication in chronic wound infections [10].

Despite the promising biomedical potential of AgNPs, chemical and physical methods of nanoparticle synthesis often involve toxic reducing agents, high energy input, or environmentally hazardous solvents, raising concerns about safety and sustainability. To address these issues, green synthesis methods have emerged as a sustainable and eco-friendly alternative. These approaches utilize biological materials such as plant extracts, microorganisms, or enzymes to reduce metal ions into nanoparticles, typically under mild conditions and without the need for hazardous reagents [11].

Plant-mediated synthesis, in particular, offers multiple advantages. Plants contain a diverse array of secondary metabolites—flavonoids, alkaloids, terpenoids, phenolics, and sugars—that not only act as reducing agents but also stabilize the nanoparticles by capping their surfaces [12]. Among various plant-derived materials, citrus fruit peels, especially from *Citrus sinensis* (orange), are of particular interest due to their high content of vitamin C, citric acid, limonoids, flavonoids like hesperidin and naringin, and essential oils [13,14]. These bioactive compounds can effectively reduce silver ions (Ag^+) to elemental silver (Ag^o) while also providing biocompatibility and additional therapeutic benefits. Moreover, the use of orange peels represents a value-added approach to agricultural waste management, aligning with the principles of green chemistry and circular economy.

Previous studies have demonstrated the antimicrobial activity of green-synthesized AgNPs against a range of bacteria, including resistant strains [15,16]. However, few investigations have focused specifically on the clinical relevance of such nanoparticles against pathogenic bacteria isolated directly from patients with burn and wound infections, which are among the most difficult infections to treat. Furthermore, the unique physicochemical characteristics of AgNPs — including particle size, morphology, crystallinity, and surface chemistry — greatly influence their biological activity and must be thoroughly characterized using advanced techniques such as UV-Vis spectroscopy, X-ray diffraction (XRD), transmission electron microscopy (TEM), and Fourier-transform infrared spectroscopy (FTIR) [17].

The present study addresses this gap by synthesizing silver nanoparticles using orange peel extract via a green synthesis route and evaluating their antimicrobial efficacy against clinical isolates from burn and wound infections, including MDR strains. The study further characterizes the synthesized nanoparticles to understand their structural and functional properties. The findings contribute to the development of sustainable nanotechnological solutions and offer promising

insights for future antimicrobial therapeutics in clinical microbiology.

MATERIALS AND METHODS

Study Design

This study was conducted in two distinct phases: a cross-sectional phase and an experimental phase. During the cross-sectional phase, clinical samples were collected and pathogenic bacteria were isolated and identified. The experimental phase focused on the green synthesis and characterization of silver nanoparticles (AgNPs) using orange peel extract and the evaluation of their antibacterial effects against both standard and multidrug-resistant (MDR) bacterial strains isolated from the burn and wound infections.

Study Population

The target population in this study consisted of bacterial strains isolated from patients with burn and wound infections. A total of 150 clinical samples were collected from patients admitted to healthcare centers during the study period. These samples were collected under sterile conditions from patients who had not received recent antibiotic therapy to avoid interference in bacterial isolation. Samples were excluded if they originated from environmental or non-infectious sources.

In the experimental phase, 12 bacterial strains showing multidrug resistance (MDR) were selected from the pool of isolates for testing the antimicrobial effects of biosynthesized AgNPs. In addition, standard bacterial strains were also included for comparison.

Sample Collection and Bacterial Identification

One hundred and fifty wound and burn specimens were collected using sterile swabs from patients and immediately transferred into Brain Heart Infusion (BHI) broth for enrichment and transport. The initial culture and primary identification of bacterial strains were performed by trained personnel in the microbiology laboratory of the hospital. To confirm the preliminary identification, further microbiological and biochemical tests were conducted, including Gram staining and culture on Blood agar and Eosin Methylene Blue (EMB) agar. Additional biochemical tests, such as oxidase, catalase, IMViC, coagulase, and sugar fermentation tests, were carried out for species-level identification. All confirmed isolates were preserved at –20°C in 18% (v/v) glycerol for future analysis.

Preparation of Orange Peel Extract

Fresh orange peels were collected and washed thoroughly with distilled water to remove surface contaminants. The cleaned peels were then dried in a well-ventilated area or at a low temperature in a hot air oven to prevent the degradation of bioactive compounds. Once completely dried, the peels were ground into a fine powder using a sterile grinder. Ten grams of the powder were mixed with 100 mL of distilled water and heated at a controlled temperature between 60°C and 90°C for 30 minutes with continuous stirring. After the extraction process, the mixture was allowed to cool and filtered using Whatman filter paper to obtain a clear extract. The resulting orange peel extract was stored at 4°C for later use in nanoparticle synthesis.

Biosynthesis of Silver Nanoparticles

Silver nanoparticles were synthesized using the aqueous extract of orange peel as the reducing and capping agent, with silver nitrate ($AgNO_3$) serving as the precursor. A stock solution of $AgNO_3$ (1 mM) was prepared by dissolving 0.169 g of $AgNO_3$ in 1000 mL of deionized water. The biosynthesis process was optimized by altering several parameters, including extract-to-$AgNO_3$ ratio, pH, reaction temperature, and incubation time, in order to achieve nanoparticles with optimal size, stability, and morphology. Optimization parameters for biosynthesis of AgNPs has been shown in Table 1.

During the reaction, the formation of AgNPs was indicated by a color change of the solution from orange to dark brown due to surface plasmon

Table 1. Optimization parameters for biosynthesis of silver nanoparticles.

Parameter	Tested Conditions
Extract-to-$AgNO_3$ ratio	1:1, 1:2, 1:3, 1:5, 1:10 (v/v)
pH	6, 7, 8, 9 (adjusted using NaOH or HCl)
Temperature	Room temperature, 60°C, 80°C
Reaction time	30 min, 1 h, 2 h, 24 h

resonance. The reaction mixture was stirred continuously at controlled temperatures (60–90°C) for one to two hours. The optimized conditions were determined by visual inspection and later confirmed by characterization techniques.

Characterization of Silver Nanoparticles

The biosynthesized AgNPs were characterized to determine their optical, structural, and morphological properties. UV-visible spectroscopy (UV-Vis) was performed using a METASH UV-9600A double-beam spectrophotometer across the 300–600 nm wavelength range to confirm nanoparticle formation by detecting surface plasmon resonance.

Fourier-Transform Infrared Spectroscopy (FTIR) was employed to identify functional groups in the orange peel extract and on the surface of AgNPs using the KBr pellet technique within the range of 400–4000 cm^{-1}. This helped determine the biomolecules responsible for reduction and stabilization.

X-ray Diffraction (XRD) analysis was conducted to evaluate the crystallinity of dried AgNP powder. The XRD patterns were recorded in the 2θ range of 30° to 90° using Cu Kα radiation, and the average crystallite size was calculated using the Scherrer equation.

Transmission Electron Microscopy (TEM) was used to determine the size, morphology, and dispersion of the synthesized AgNPs. A drop of the AgNP solution was placed on a carbon-coated copper grid and air-dried. Images were captured at 300 kV, and at least 100 nanoparticles were measured using image analysis software to estimate the size distribution.

Zeta Potential and DLS Analysis

To determine the surface charge and stability of the AgNPs, zeta potential analysis was carried out using a Malvern Zetasizer ZS 90. A 100 µg/mL AgNP suspension in Luria broth containing 0.05% NaCl was incubated at 32°C and 37°C with shaking at 225 rpm, and 1 mL samples were collected every 2 hours for analysis. Additionally, dynamic light scattering (DLS) was conducted using a Horiba SZ-100 nanoparticle analyzer to assess the particle size distribution and dispersity.

Isolation and Identification of Pathogenic Bacteria

Bacterial isolates were obtained from clinical samples collected between December 2024 and June 2025 from patients suffering from burn and wound infections. The samples were collected using sterile swabs from infected sites and transported to the microbiology laboratory under sterile conditions. Swabs were cultured on a variety of media, including nutrient agar, blood agar, MacConkey agar, mannitol salt agar, and Pseudomonas isolation agar. Plates were incubated at 37°C for 24–48 hours. Colonies with distinct morphology were subjected to Gram staining and a series of biochemical tests such as catalase, coagulase, oxidase, IMViC tests, and sugar fermentation tests for bacterial identification.

Antimicrobial Susceptibility Testing

The antimicrobial resistance profiles of the isolated strains were evaluated using the Kirby-Bauer disk diffusion method, according to Clinical and Laboratory Standards Institute (CLSI, 2024) guidelines. A range of commonly used antibiotic discs was applied to determine the resistance spectrum of the isolates. Antibiotics tested included agents from various classes such as beta-lactams, aminoglycosides, fluoroquinolones, macrolides, and carbapenems. The results were interpreted by measuring the diameter of inhibition zones and comparing them with CLSI standards.

Identification of Multidrug-Resistant Strains

Isolates exhibiting resistance to at least one agent in three or more antimicrobial classes were classified as multidrug-resistant (MDR). The identification of MDR strains was based on the results of antimicrobial susceptibility testing. This classification follows international guidelines and reflects the clinical challenge posed by such strains in therapeutic settings.

Evaluation of Antibacterial Activity of AgNPs

The antibacterial activity of the biosynthesized AgNPs was evaluated against both MDR isolates and standard bacterial strains. The minimum inhibitory concentration (MIC) of AgNPs was determined using the broth microdilution method. A series of twofold serial dilutions of AgNPs ranging from 512 to 0.5 µg/mL were prepared in cation-adjusted Mueller-Hinton broth (CAMHB). Each well of a 96-well microtiter plate received 100 µL of bacterial inoculum (~1.5×10^6 CFU/mL) and 100 µL of AgNP solution.

The plates were incubated for 24 hours at

35 ± 2°C. MICs were determined visually as the lowest concentration of AgNPs that prevented visible bacterial growth. Spectrophotometric measurements at 600 nm (OD_{600}) were used to confirm inhibition, with OD values ≤ 0.1 considered indicative of microbial growth suppression. The MICs of the biosynthesized AgNPs were compared with those of standard antibiotics and commercially available AgNPs to evaluate their relative efficacy against MDR and standard bacterial strains.

Statistical analysis

For statistical analysis, we used SPSS software, version 20.0 (SPSS Inc., Chicago, IL, USA), and Minitab software version 16.2.0. In the current study, quantitative variables in descriptive objectives was estimated based on mean and standard deviation, and qualitative variables was estimated by number and percentage. Also, parametric tests (t-test, ANOVA) and non-parametric equivalent tests (chi-square, Kruskal-Wallis, Mann-Whitney, etc.) was used for analytical purposes and hypotheses if normality assumptions are established. A p-value of less than 0.05 was considered statistically significant.

RESULTS AND DISCUSSION

Collection of Samples and Identification of Bacterial Isolates

A total of 150 clinical isolates were collected from patients with a mean age of 61.4 ± 20.43 years, ranging from 1 to 93 years. Of these patients, 94 (62.6%) were male and 56 (37.3%) were female. The majority of the isolates (118, 78.6%) were obtained from burn wounds, while 32 (21.3%) were collected from other wound infections, including surgical and traumatic wounds.

Microbiological analysis identified 55 isolates (36.6%) as *Pseudomonas aeruginosa*, 8 (5.3%) as *Acinetobacter baumannii*, and 8 (8%) as *Klebsiella pneumoniae* among the Gram-negative strains. From the Gram-positive group, 41 isolates (27.3%) were identified as *Staphylococcus epidermidis* and 34 (22.6%) as *Staphylococcus aureus*. No *Enterococcus faecalis* was isolated from the clinical specimens. For the purpose of antimicrobial activity testing, 10 multidrug-resistant (MDR) clinical isolates were selected, in addition to 6 standard strains, including *S. aureus* ATCC 33591, *S. epidermidis* ATCC 12228, *E. faecalis* ATCC 19433, *K. pneumoniae* ATCC 700603, *A. baumannii* ATCC 19606, and *P. aeruginosa* ATCC 27853.

Antimicrobial Susceptibility Profile

The Gram-negative isolates exhibited high resistance rates against several antibiotics, particularly meropenem, imipenem, ciprofloxacin, amikacin, and ceftriaxone. Specifically, multidrug resistance was observed in 41 isolates (74.5%) of *P. aeruginosa*, 7 (87.5%) of *A. baumannii*, and 8 (66.6%) of *K. pneumoniae*. The detailed antibiotic resistance patterns of the Gram-negative isolates are presented in Table 2.

For the Gram-positive isolates, *S. aureus* displayed resistance to penicillin, clindamycin, azithromycin, tetracycline, amoxicillin/clavulanic acid, gentamicin, oxacillin, and rifampin. *S. epidermidis* showed high resistance against penicillin, tetracycline, erythromycin, cefazolin, and trimethoprim-sulfamethoxazole. MDR strains were detected in 35 isolates (51.2%) of *S. epidermidis* and 25 isolates (73.5%) of *S. aureus*. These findings are summarized in Table 3.

Green Biosynthesis of AgNPs Using Orange Peel Extract

The biosynthesis of silver nanoparticles (AgNPs) was visually confirmed by a gradual color change of the reaction solution from orange to brown, indicating the reduction of silver ions (Ag^{+}) to metallic silver (Ag^{0}) by the bioactive compounds in orange peel extract. This extract functioned both as a reducing and a stabilizing agent in the green

Table 2. Antimicrobial susceptibility testing for nonduplicated isolates of *Pseudomonas aeruginosa*, *Klebsiella pneumoniae* and *Acinetobacter baumannii* strains isolated over study period.

	CIP		GM		CAZ		CRO		CTX		AMS		CPM		AN		CS		IPM		MEM	
Bacteria	R	S	R	S	R	S	R	S	R	S	R	S	R	S	R	S	R	S	R	S	R	S
P. aeruginosa (n=55)	55	0	53	2	50	5	49	6	52	3	54	1	54	1	48	7	5	50	55	0	55	0
K. pneumoniae (n=12)	12	0	12	0	10	2	12	0	12	0	12	0	12	0	10	2	0	12	12	0	11	1
A. baumannii (n=8)	8	0	8	0	7	1	8	0	8	0	8	0	8	0	7	1	1	7	8	0	7	1

CRO: ceftriaxone, CTX: cefotaxime, AMS: amoxicillin, CPM: cefepime, AN: amikacin, CAZ: ceftazidime, CIP: ciprofloxacin, GM: gentamicin and CS: colistin; IPM: Imipenem; MEM: Meropenem

synthesis process.

Characterization of Biosynthesized AgNPs

UV-Vis Spectroscopy

The successful synthesis of AgNPs was verified using UV-Vis spectroscopy. The characteristic surface plasmon resonance (SPR) peak was observed at 418 nm after 24 hours of incubation at room temperature (27°C) and pH 9.0, confirming nanoparticle formation. The increase in SPR absorbance over time and extract concentration further supported the role of phytochemicals in facilitating the reduction process. Fig. 1 illustrates the visual and spectral confirmation of AgNP formation.

X-Ray Diffraction (XRD)

XRD analysis demonstrated crystalline nature of the biosynthesized AgNPs. The diffraction peaks observed at 2θ values of 38.10°, 44.22°, 64.44°, and 77.37° corresponded to the (111), (200), (220), and (311) planes of the face-centered cubic structure of silver. These findings matched the standard reference JCPDS card (No. 04-0679), confirming the high crystallinity of the particles. Fig. 2 presents the XRD pattern.

Transmission Electron Microscopy (TEM)

TEM imaging revealed that the AgNPs were predominantly spherical and polydisperse, with particle sizes ranging from 10 to 45 nm. The average particle size was estimated to be 24.5 nm. Selected Area Electron Diffraction (SAED) patterns indicated the crystalline nature of the nanoparticles. The particles were well-dispersed with minimal agglomeration, as shown in Fig. 3.

Table 3. Antimicrobial susceptibility testing for nonduplicated isolates of *S. aureus* and *S. epidermidis* strains isolated over study period.

	P		CL		AZ		TE		ET		AMC		GE		OXA		RIF		CZ		SXT	
Bacteria	R	S	R	S	R	S	R	S	R	S	R	S	R	S	R	S	R	S	R	S	R	S
S. epidermidis (n=41)	40	1	39	2	33	8	39	2	38	3	-	-	26	15	-	-	5	50	55	0	28	13
S. aureus (n=34)	34	0	29	5	27	7	26	8	-	-	29	5	26	8	21	13	12	22	-	-	-	-

P: penicillin, CL: clindamycin, AZ: azithromycin, TE: tetracycline, ET: erythromycin, AMC: amoxicillin/clavulanic, GE: gentamicin, OXA: oxacillin, RIF: rifampin; CZ: cefazolin; SXT: trimethoprim-sulfamethoxazole

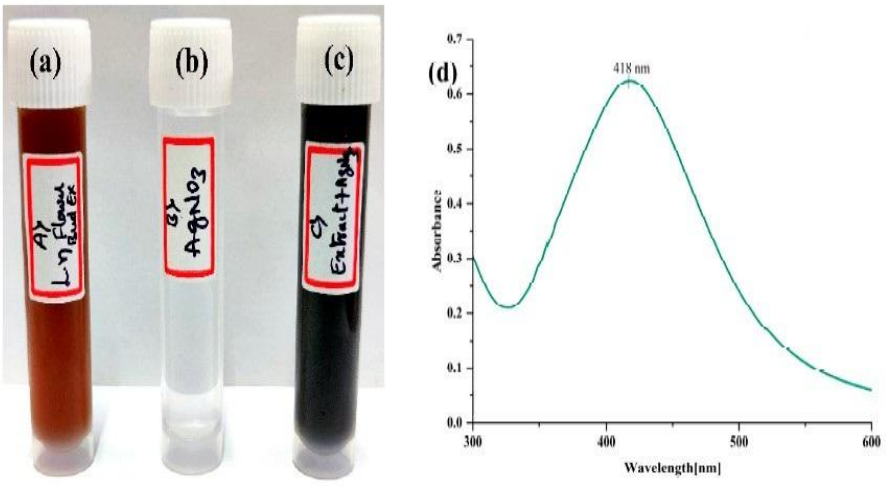

Fig. 1. Change in color of the solution: (a) orange peel extract; (b) $AgNO_3$ solution; (c) orange peel extract + $AgNO_3$; (d) UV-Vis absorption spectrum of biosynthesized AgNPs from orange peel extract. The UV analysis of orange peel extract - synthesized AgNPs, which reveals a significant peak at 418 nm.

Fourier-Transform Infrared Spectroscopy (FTIR)

FTIR spectra of the orange peel extract and synthesized AgNPs indicated the presence of functional groups such as hydroxyl, carbonyl, carboxyl, and amine groups. These groups played a critical role in the reduction and stabilization of AgNPs. Shifts in peak positions between the spectra confirmed the interaction of biomolecules with silver ions. The comparative spectra are presented in Fig. 4.

Zeta Potential and Dynamic Light Scattering (DLS) Analysis

The zeta potential measurement showed

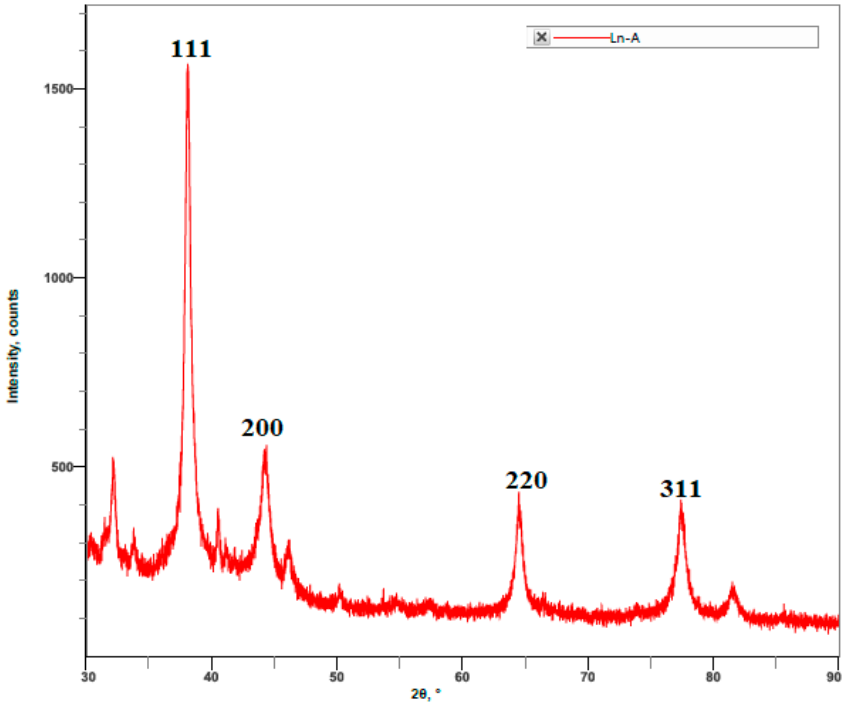

Fig. 2. XRD spectra of biosynthesized AgNPs from orange peel extract.

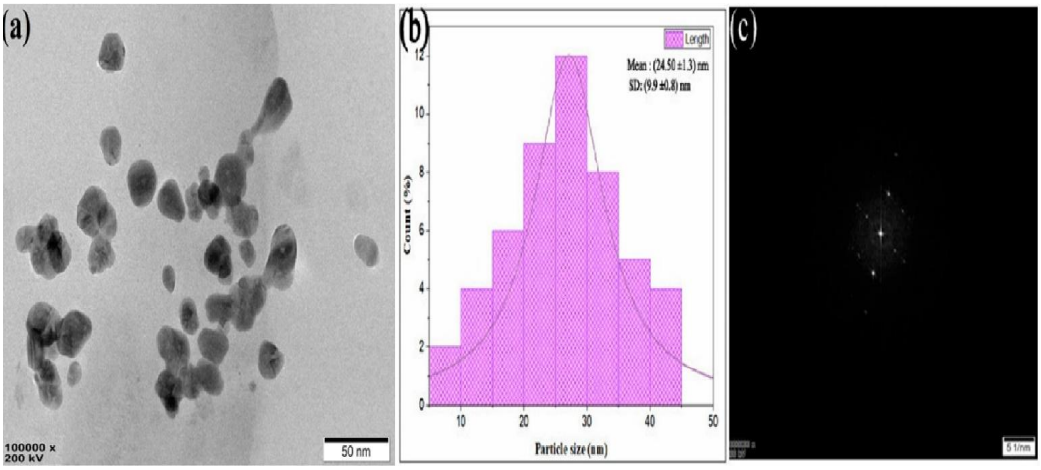

Fig. 3. (a) TEM image, (b) histogram showing particle size distribution, and (c) SAED pattern image of biosynthesized AgNPs from orange peel extract.

a highly negative surface charge of −31.4 mV, indicating strong electrostatic stability and good dispersion in colloidal form (Fig. 5a). DLS analysis revealed an average hydrodynamic diameter of 98.5 nm, larger than the TEM-measured size, due to the surrounding phytochemical corona (Fig. 5b). These results confirm the stable and well-dispersed nature of the synthesized AgNPs.

Antimicrobial Activity of AgNPs

The antimicrobial activity of the synthesized AgNPs was assessed using both disk diffusion and broth microdilution methods. Disk diffusion tests revealed significant inhibition zones for most tested strains. The greatest zones of inhibition were observed against *S. epidermidis*, *S. aureus*, and *P. aeruginosa* (33 ± 0.8 mm, 33 ± 0.2 mm, and 31 ± 1 mm, respectively). *A. baumannii* and *K. pneumoniae* showed slightly lower sensitivity, with zones measuring 27 ± 0.7 mm and 28 ± 0.5 mm. The inhibition zones are shown in Fig. 6.

Broth microdilution assays demonstrated potent antibacterial effects of the AgNPs at low MIC values. The lowest MIC was recorded for *S. aureus* ATCC 33591 (25 µg/mL), which also showed the largest inhibition zone (35 mm). Other MDR strains, including *S. epidermidis*, *S. aureus*, *P. aeruginosa*, and *K. pneumoniae*, exhibited significant susceptibility. *P. aeruginosa* ATCC 33591 was the least sensitive with a MIC of 125 µg/mL. No antibacterial activity was observed for the orange peel extract alone, used as a control. Detailed MIC values and inhibition zone diameters are presented in Table 4.

The increasing interest in environmentally benign approaches to nanoparticle synthesis has brought plant-mediated methods to the forefront of nanobiotechnology. Plant-based materials are typically non-toxic, renewable, and rich in phytochemicals, making them ideal candidates for green synthesis processes [18]. In this study, we successfully synthesized silver nanoparticles (AgNPs) using orange peel extract—an agricultural waste product often discarded without further

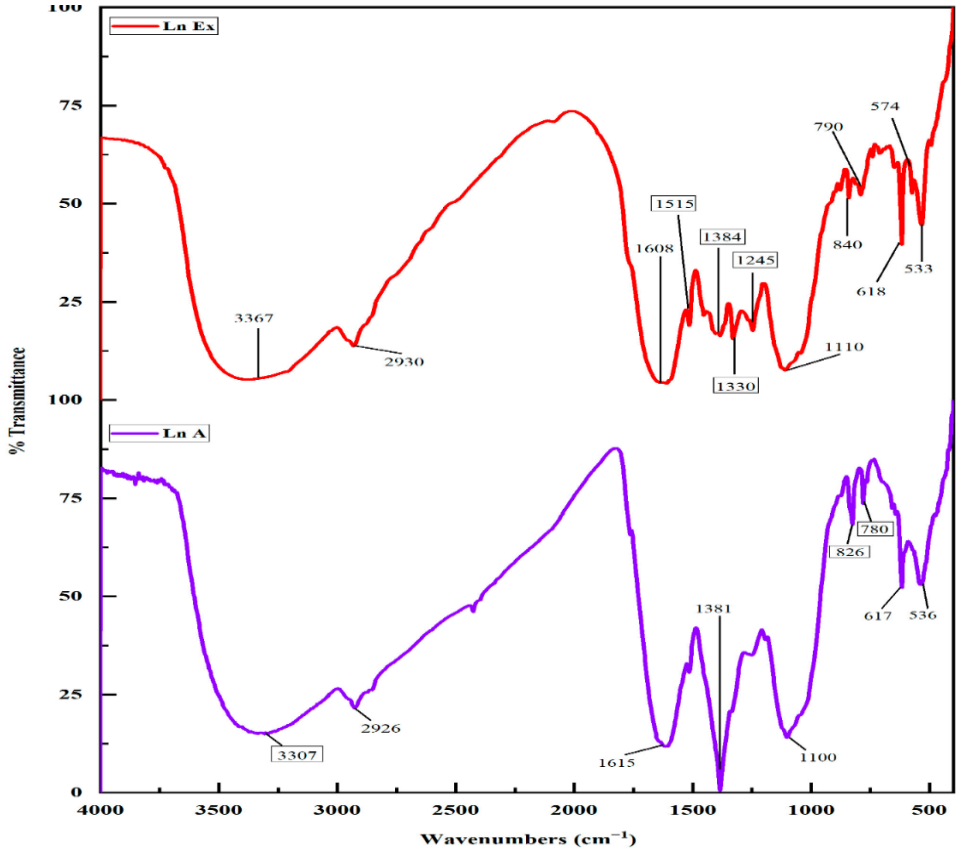

Fig. 4. FTIR spectrum of AgNPs synthesized from orange peel extract.

use. This not only enhances the sustainability of the process but also introduces a novel method, as orange peel is infrequently employed in AgNP biosynthesis, underscoring the originality of our approach.

The visible transformation of the solution's color from orange to brown was the first indication of AgNP formation, attributed to the surface plasmon resonance (SPR) phenomenon that occurs when silver ions are reduced to metallic nanoparticles. UV-Vis spectroscopy confirmed this by detecting a distinct absorption peak at 418 nm, within the typical range for AgNPs (400–450 nm), thereby affirming the successful synthesis of AgNPs using orange peel extract.

Orange peel extract served as both a reducing and stabilizing agent, a dual role made possible by its phytochemical composition, which includes

Peak No	Zeta potential	Electrophoretic mobility
1	-31.4 mV	-0.000243 cm²/Vs
2	--- mV	---------- cm²/Vs
3	--- mV	---------- cm²/Vs

Zeta Potential (Mean) : -31.4 mV
Electrophoretic Mobility Mean : -0.000243 cm²/Vs

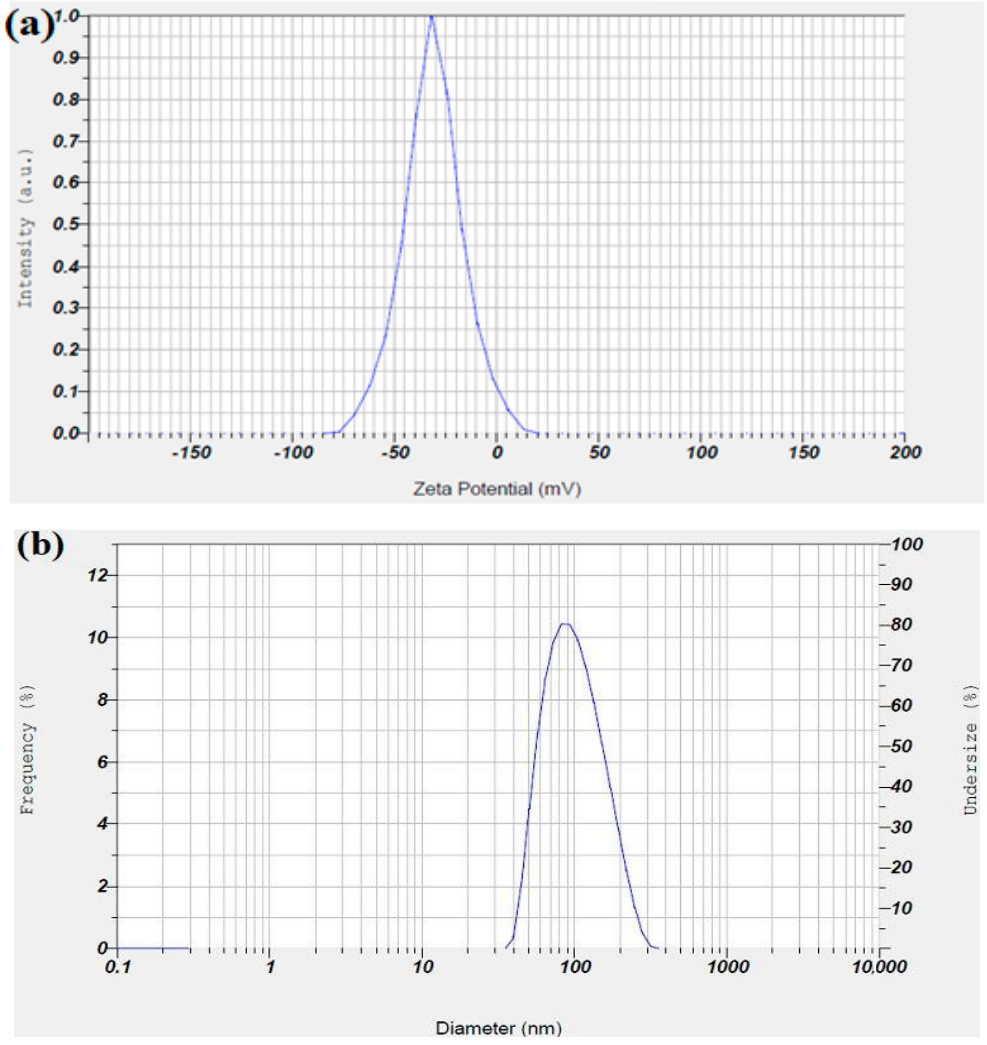

Fig. 5. (a) Zeta potential analysis graph and (b) dynamic light scattering analysis of biosynthesized AgNPs from orange peel extract.

flavonoids, phenolic acids, and essential oils. These biomolecules facilitate the reduction of silver ions (Ag^+) to elemental silver (Ag^0) while concurrently stabilizing the formed nanoparticles to prevent aggregation. Compared to other green synthesis methods—such as those using *Aloe vera* where acemannan acts as the key bioactive molecule—our approach relies on a different phytochemical matrix, potentially imparting unique characteristics to the resulting nanoparticles [19].

X-ray diffraction (XRD) analysis revealed Bragg reflection peaks corresponding to the (111), (200), (220), and (311) planes of a face-centered cubic (FCC) crystalline structure, verifying the formation of crystalline silver nanoparticles. This crystallinity is essential for the functional properties of AgNPs, particularly their antimicrobial activity. Transmission electron microscopy (TEM) showed that the nanoparticles were predominantly spherical and polydisperse, with sizes ranging from 10 to 45 nm and an average diameter of 24.5 nm. While some aggregation was noted—likely due to incomplete stabilization by biomolecules—this size range falls within the optimal window for effective antimicrobial activity. Notably, our nanoparticles were smaller than those synthesized using polystyrene nanocomposites (98.43 nm) (20) or bacterial synthesis (30–70 nm) (126), potentially explaining their superior bioactivity.

Fourier-transform infrared spectroscopy (FTIR) analysis revealed peaks corresponding to hydroxyl (-OH), carbonyl (C=O), carboxyl (-COOH), and amine ($-NH_2$) functional groups. These groups originate from orange peel biomolecules and are crucial for both reduction and stabilization. Their interaction with AgNPs also imparts surface functionality, which can influence biological interactions, especially antimicrobial efficacy. Zeta potential analysis revealed a highly negative value (-31.4 mV), indicating strong electrostatic repulsion between particles, which correlates with good colloidal stability. The stability was further confirmed by dynamic light scattering (DLS), which showed a hydrodynamic diameter of ~98.5 nm—larger than the TEM results due to the hydration shell surrounding the particles. Such size discrepancies are typical and underscore the importance of using complementary characterization techniques.

From a clinical standpoint, this study's focus on multidrug-resistant (MDR) bacterial isolates—notably *P. aeruginosa* (74.5%), *K. pneumoniae* (66.6%), and *A. baumannii* (87.5%)—from burn and wound infections demonstrates the pressing need for novel antimicrobial strategies. These Gram-negative pathogens, along with resistant Gram-positive strains like *S. aureus* (73.5%) and *S. epidermidis* (51.2%), highlight the

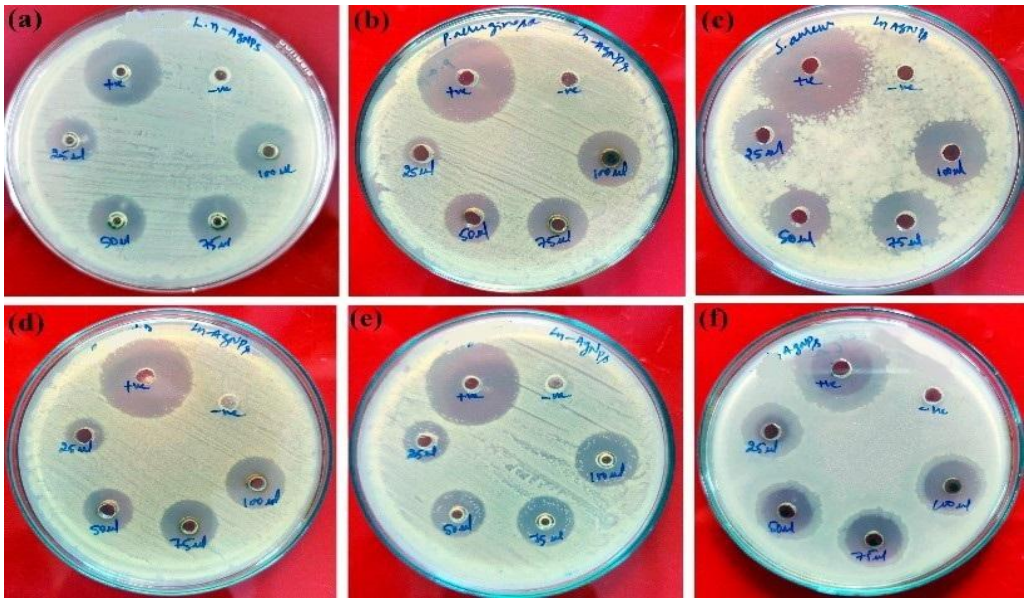

Fig. 6. Antimicrobial activity of biosynthesized AgNPs against the study isolates.

global healthcare challenge posed by antibiotic resistance. Resistance to broad-spectrum agents such as meropenem, imipenem, and ceftriaxone reflects the diminishing arsenal of effective antibiotics.

The antimicrobial activity of AgNPs, assessed via disk diffusion and broth microdilution assays, showed significant inhibition against both Gram-positive and Gram-negative MDR strains. *S. aureus* ATCC 33591 exhibited the largest inhibition zone (35 mm at 1000 µg/mL), with a minimum inhibitory concentration (MIC) of just 25 µg/mL. This efficacy mirrors or surpasses those reported in studies using *Aloe vera*-based AgNPs, which achieved inhibition zones of 21 mm against *S. aureus* [19]. In this study, Gram-positive strains were generally more susceptible to AgNPs, possibly due to the lack of an outer membrane, which in Gram-negative bacteria serves as a barrier to nanoparticle penetration. The antimicrobial mechanisms of AgNPs include cell membrane disruption, ROS generation, and interference with DNA/protein synthesis. These nanoparticles can attach to bacterial membranes, penetrate cells, and cause intracellular damage—contributing to bacteriostasis or bactericidal effects [21]. Our findings suggest that these biosynthesized AgNPs could serve as a potent alternative or adjunct to antibiotics, especially for topical applications on burn wounds where resistance is rampant.

Environmental parameters such as temperature and salinity were shown to affect AgNP stability and antimicrobial efficacy. Agglomeration was more pronounced at higher salt concentrations and lower temperatures, leading to larger particles and diminished activity. Conversely, the optimal conditions for stability were found at 32°C and 0.05% NaCl, consistent with environmental conditions in some natural and clinical settings. This points to the critical role of physicochemical parameters in determining nanoparticle behavior and biological activity [22-24]. Our study aligns with others showing that size is a major determinant of antibacterial effectiveness. Smaller nanoparticles (~9.3 nm) exhibit stronger antimicrobial effects due to a larger surface area-to-volume ratio, which enhances interaction with bacterial cells (25). Our 24 nm AgNPs showed comparable MIC values

Table 4. The results of the antimicrobial assays performed to evaluate the activity of the green-synthesized AgNPs against the bacterial isolates.

	AgNPs		Ciprofloxacin	Gentamycin	orange peel extract
Bacterial Strain	Zone of Inhibition (mm)	MIC	Zone of Inhibition (mm)	Zone of Inhibition (mm)	Zone of Inhibition (mm)
MDR *S. epidermidis*	33	50	12	11	ND
S. epidermidis ATCC 12228	30	50	11	12	ND
MDR *P. aeruginosa*	31	100	ND	7	ND
P. aeruginosa ATCC 33591	25	125	12	15	ND
MDR *A. baumannii,*	27	100	10	10	ND
A. baumannii ATCC 19606	28	100	12	11	ND
MDR K. pneumonia	28	50	10	12	ND
K. pneumoniae ATCC 700603	30	50	39	18	ND
MDR *S. aureus*	33	25	11	12	ND
S. aureus ATCC 33591	35	25	15	12	ND
E. faecalis ATCC 19433	30	50	12	10	ND

ND: Not detected

to those in the literature, reinforcing that size-dependent toxicity is a key factor in nanoparticle-mediated antimicrobial activity [25-27].

AgNPs are increasingly acknowledged as viable antimicrobial agents in biomedical applications, especially in wound care. Commercial products like Acticoat™ utilize silver compounds for their potent antimicrobial effects. Unlike antibiotics, bacteria have not yet developed significant resistance mechanisms against AgNPs, making them promising for long-term use.

Despite the compelling findings, several limitations must be acknowledged. The number of clinical isolates for some species (e.g., *A. baumannii*, *K. pneumoniae*) was relatively low, limiting statistical power. Furthermore, the specific resistance genes were not identified, which could provide insight into resistance mechanisms. The study remains in vitro, and the lack of in vivo data leaves open questions about cytotoxicity, biocompatibility, and systemic efficacy. Also, *E. faecalis* was not isolated in our study, despite being a common pathogen in similar infections.

CONCLUSION

This study highlights the green synthesis of AgNPs using orange peel extract as a novel and sustainable approach. The synthesized nanoparticles were characterized as stable, bioactive, and potent against multidrug-resistant (MDR) bacteria, particularly Gram-positive strains. The findings not only contribute to the development of eco-friendly nanotechnology but also provide promising alternatives to conventional antibiotics in the fight against rising antimicrobial resistance. Future research should focus on in vivo applications, molecular resistance mechanisms, and environmental interactions to fully harness the potential of AgNPs in medical and ecological settings.

CONFLICT OF INTEREST

The authors declare that there is no conflict of interests regarding the publication of this manuscript.

REFERENCES

1. Church D, Elsayed S, Reid O, Winston B, Lindsay R. Burn Wound Infections. Clin Microbiol Rev. 2006;19(2):403-434.
2. Rowan MP, Cancio LC, Elster EA, Burmeister DM, Rose LF, Natesan S, et al. Burn wound healing and treatment: review and advancements. Critical Care. 2015;19(1).
3. Branski LK, Al-Mousawi A, Rivero H, Jeschke MG, Sanford AP, Herndon DN. Emerging Infections in Burns. Surg Infect (Larchmt). 2009;10(5):389-397.
4. Mendelson M, Matsoso MP. The World Health Organization Global Action Plan for antimicrobial resistance. S Afr Med J. 2015;105(5):325.
5. WITHDRAWN: Study of Biofilm Formation and Antibiotic Resistant Profile in Multidrug Resistant and Extensive Drug Resistance Pseudomonas Aeruginosa Isolated from Burn Wound Infections in Southwest Iran. Springer Science and Business Media LLC; 2021.
6. Taneja N, Emmanuel R, Chari PS, Sharma M. A prospective study of hospital-acquired infections in burn patients at a tertiary care referral centre in North India. Burns. 2004;30(7):665-669.
7. Schalk E, Färber J, Fischer T. Multidrug-Resistant Gram-Negative Bacteria in Hematology and Oncology. Infection Control and Hospital Epidemiology. 2014;35(9):1203-1204.
8. Rai M, Yadav A, Gade A. Silver nanoparticles as a new generation of antimicrobials. Biotechnol Adv. 2009;27(1):76-83.
9. Durán N, Marcato PD, Conti RD, Alves OL, Costa FTM, Brocchi M. Potential use of silver nanoparticles on pathogenic bacteria, their toxicity and possible mechanisms of action. J Braz Chem Soc. 2010;21(6):949-959.
10. Singh R, Smitha MS, Singh SP. The Role of Nanotechnology in Combating Multi-Drug Resistant Bacteria. Journal of Nanoscience and Nanotechnology. 2014;14(7):4745-4756.
11. Ahmed S, Ahmad M, Swami BL, Ikram S. A review on plants extract mediated synthesis of silver nanoparticles for antimicrobial applications: A green expertise. Journal of Advanced Research. 2016;7(1):17-28.
12. Mittal AK, Chisti Y, Banerjee UC. Synthesis of metallic nanoparticles using plant extracts. Biotechnol Adv. 2013;31(2):346-356.
13. Gupta S, Choudhary DK, Sundaram S. Green Synthesis and Characterization of Silver Nanoparticles Using Citrus sinensis (Orange peel) Extract and Their Antidiabetic, Antioxidant, Antimicrobial and Anticancer Activity. Waste and Biomass Valorization. 2024;16(3):1101-1114.
14. Dhillon GS, Kaur S, Brar SK, Verma M. Green synthesis approach: extraction of chitosan from fungus mycelia. Crit Rev Biotechnol. 2012;33(4):379-403.
15. Khan SA, Shahid S, Lee C-S. Green Synthesis of Gold and Silver Nanoparticles Using Leaf Extract of Clerodendrum inerme; Characterization, Antimicrobial, and Antioxidant Activities. Biomolecules. 2020;10(6):835.
16. Bar H, Bhui DK, Sahoo GP, Sarkar P, Pyne S, Misra A. Green synthesis of silver nanoparticles using seed extract of Jatropha curcas. Colloids Surf Physicochem Eng Aspects. 2009;348(1-3):212-216.
17. Song JY, Kim BS. Rapid biological synthesis of silver nanoparticles using plant leaf extracts. Bioprocess and Biosystems Engineering. 2008;32(1):79-84.
18. Rahimnejad M, Sadeghi-Aghbash M. Zinc Phosphate Nanoparticles: A Review on Physical, Chemical, and Biological Synthesis and their Applications. Curr Pharm Biotechnol. 2022;23(10):1228-1244.
19. Awad MA, Mekhamer WK, Merghani NM, Hendi AA, Ortashi KMO, Al-Abbas F, et al. Green Synthesis, Characterization, and Antibacterial Activity of Silver/Polystyrene Nanocomposite. Journal of Nanomaterials. 2015;2015(1).
20. P R, Krishnadhas L. Anti-Diabetic Activity of Silver Nanoparticles Synthesized From The Hydroethanolic Extract of Myristica Fragrans Seeds. Springer Science and Business Media LLC; 2021.

21. Manal AA, Awatif AH, Khalid MOO, Dalia FAE, Nada EE, Lamia AA-l, et al. Silver nanoparticles biogenic synthesized using an orange peel extract and their use as an anti-bacterial agent. International Journal of Physical Sciences. 2014;9(3):34-40.
22. Prathna TC, Chandrasekaran N, Mukherjee A. Studies on aggregation behaviour of silver nanoparticles in aqueous matrices: Effect of surface functionalization and matrix composition. Colloids Surf Physicochem Eng Aspects. 2011;390(1-3):216-224.
23. Nayak D, Ashe S, Rauta PR, Kumari M, Nayak B. Bark extract mediated green synthesis of silver nanoparticles: Evaluation of antimicrobial activity and antiproliferative response against osteosarcoma. Materials Science and Engineering: C. 2016;58:44-52.
24. Pal S, Tak YK, Song JM. Does the Antibacterial Activity of Silver Nanoparticles Depend on the Shape of the Nanoparticle? A Study of the Gram-Negative Bacterium Escherichia coli. Applied and Environmental Microbiology. 2007;73(6):1712-1720.
25. Lok C-N, Ho C-M, Chen R, He Q-Y, Yu W-Y, Sun H, et al. Proteomic Analysis of the Mode of Antibacterial Action of Silver Nanoparticles. J Proteome Res. 2006;5(4):916-924.
26. Jain J, Arora S, Rajwade JM, Omray P, Khandelwal S, Paknikar KM. Silver Nanoparticles in Therapeutics: Development of an Antimicrobial Gel Formulation for Topical Use. Mol Pharm. 2009;6(5):1388-1401.
27. Xiu Z-M, Ma J, Alvarez PJJ. Differential Effect of Common Ligands and Molecular Oxygen on Antimicrobial Activity of Silver Nanoparticles versus Silver Ions. Environmental Science an2 Technology. 2011;45(20):9003-9008.